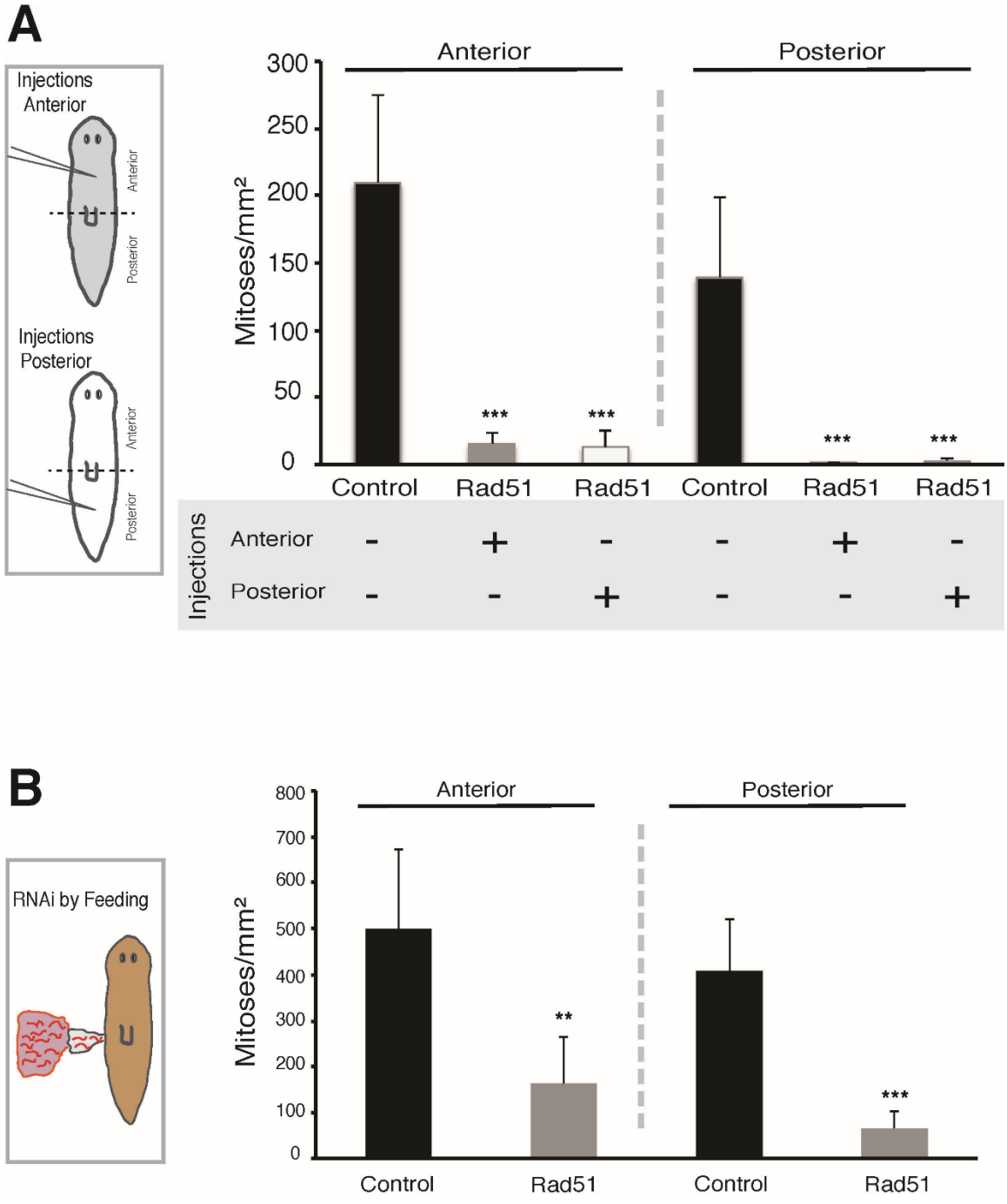

Fig. S1. Different methods of *Rad51(RNAi)* restrict cell division along the AP axis. (A) Depicts the effects of microinjections of Rad51 dsRNA in either anterior or posterior regions (represented by cartoons on the left gray and white, respectively) over mitotic activity along the AP axis. **(B)** Feeding Rad51 dsRNA synthesized *in vitro* reduces mitotic activity asymmetrically in the planarian body. Values represent mean±s.e.m. of at least two independent experiments, *n>10* animals per experiment. ****P<0.0001*, ***P<0.001* by Tukey's multiple comparison test.

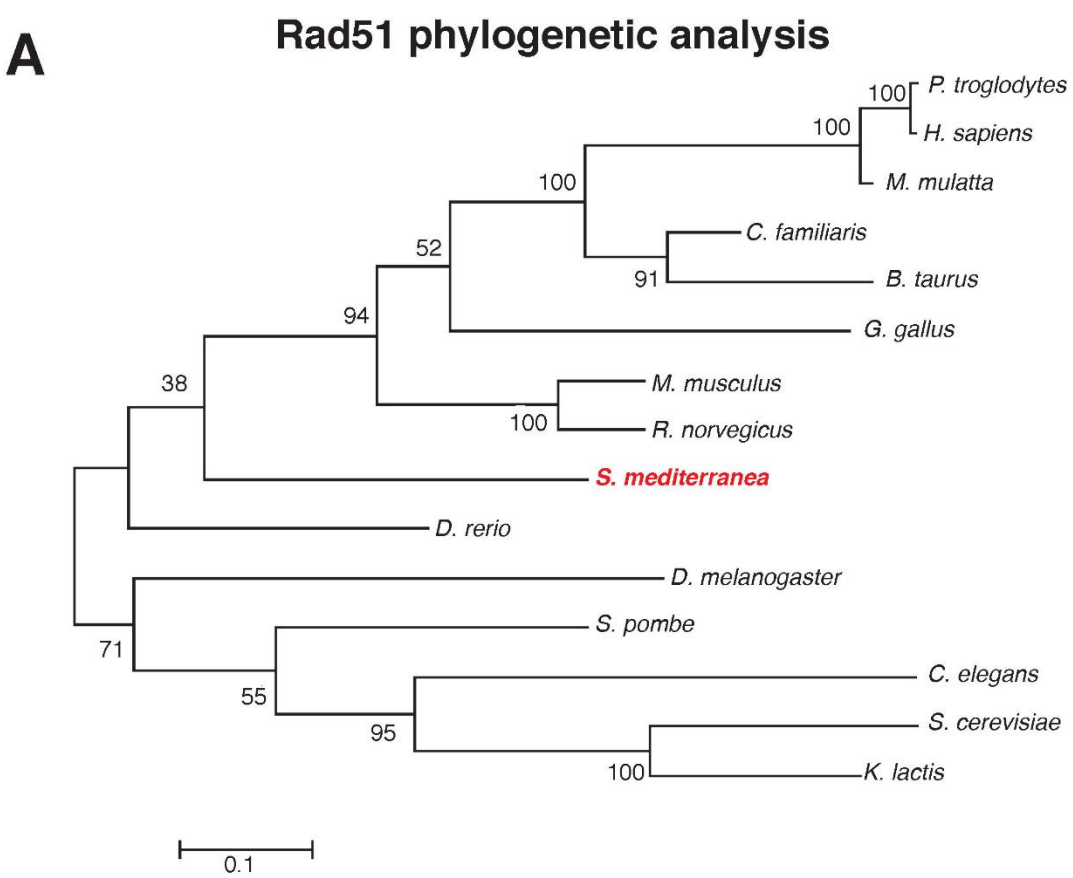

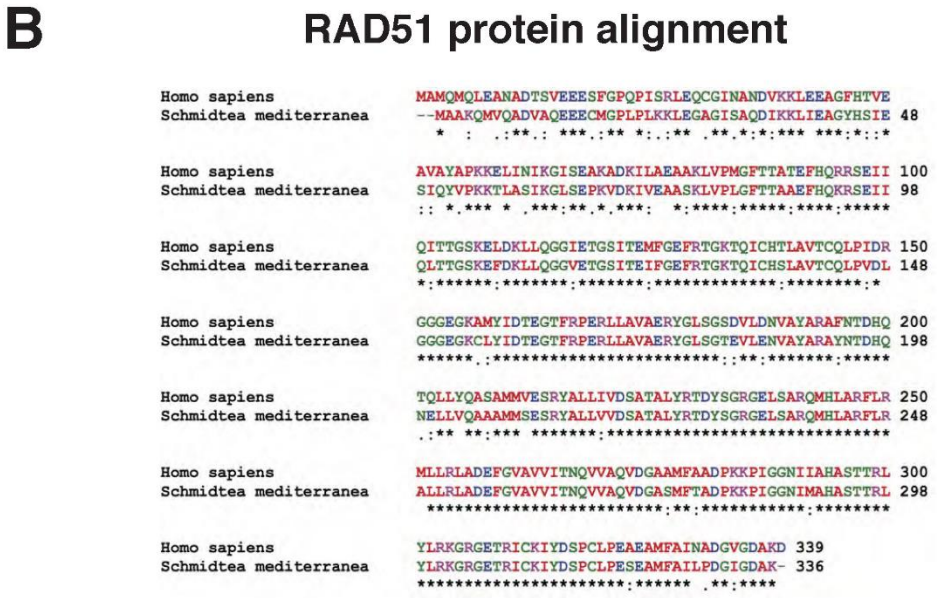

Fig. S2. The *Schmidtea mediterranea* RAD51 protein is evolutionarily and molecularly conserved. (A) Phylogenetic relationship among primates and invertebrates based on the protein sequences of RAD51. Maximum likelihood method was based on the JTT matrix-based model. The percentage of trees in which the associated taxa clustered together is shown next to the branches. The tree is drawn to scale, with branch lengths measured in the number of substitutions per site. Branch support is under 5000 Bootstrap replicas. **(B)** *S. mediterranea* and human RAD51 sequence alignments reveals sequence homology of ~90% with its human counterpart.

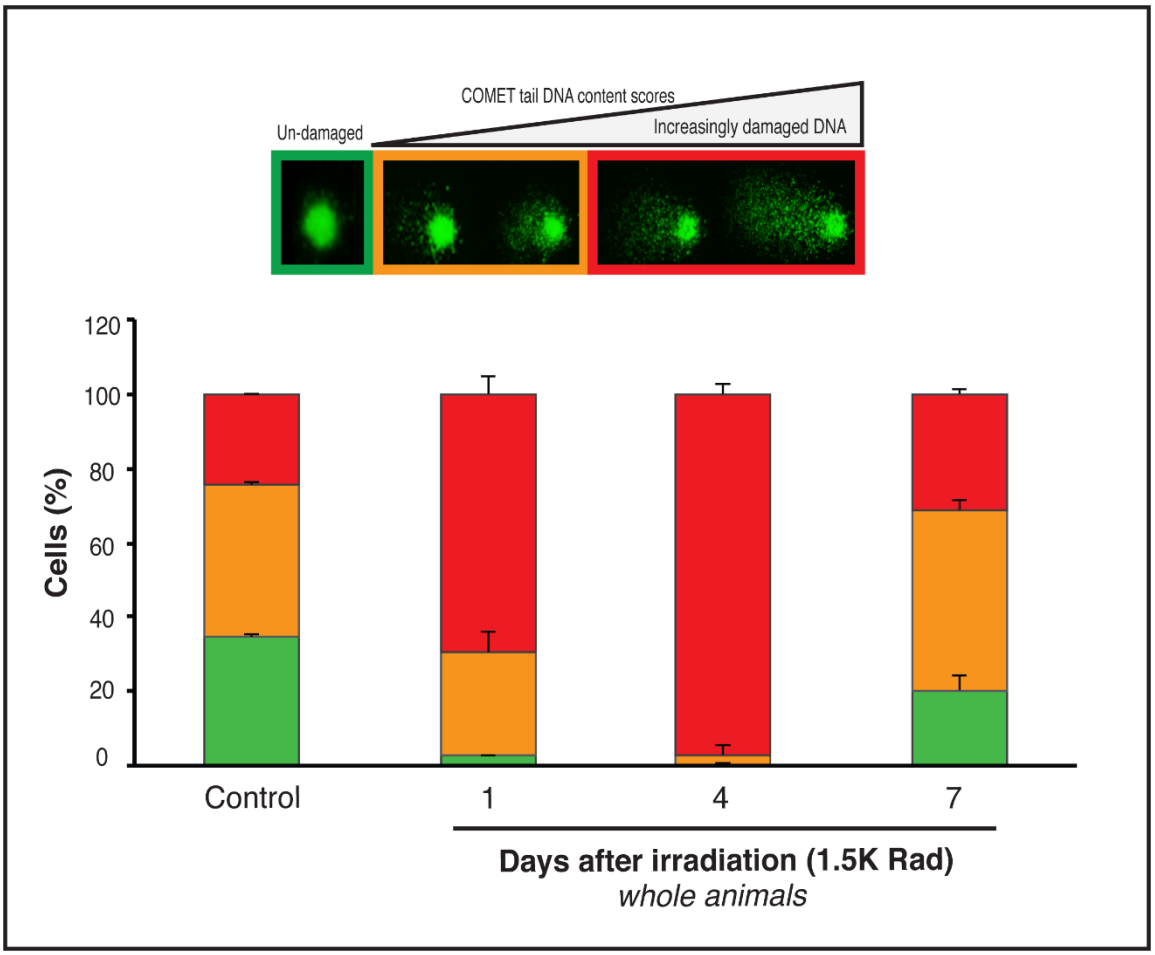

Fig. S3. **The Comet assay detects DNA damage and its repair after sublethal irradiation.** DNA damage in whole organisms assessed by the Comet assay, gel electrophoresis under alkaline conditions. Visual scoring was used to quantify DNA damage, color-coded key at top represents: undamaged (green), moderate damage (orange), and extremely damaged DNA (red) shown. Maximum DNA damage is observed by day 4 post-irradiation, but by day 7 post-irradiation there is considerable less DNA damage. Graph represents mean±s.e.m. of three independent experiments with n=10 animals each. Irradiation consisted of 1,000 rad.

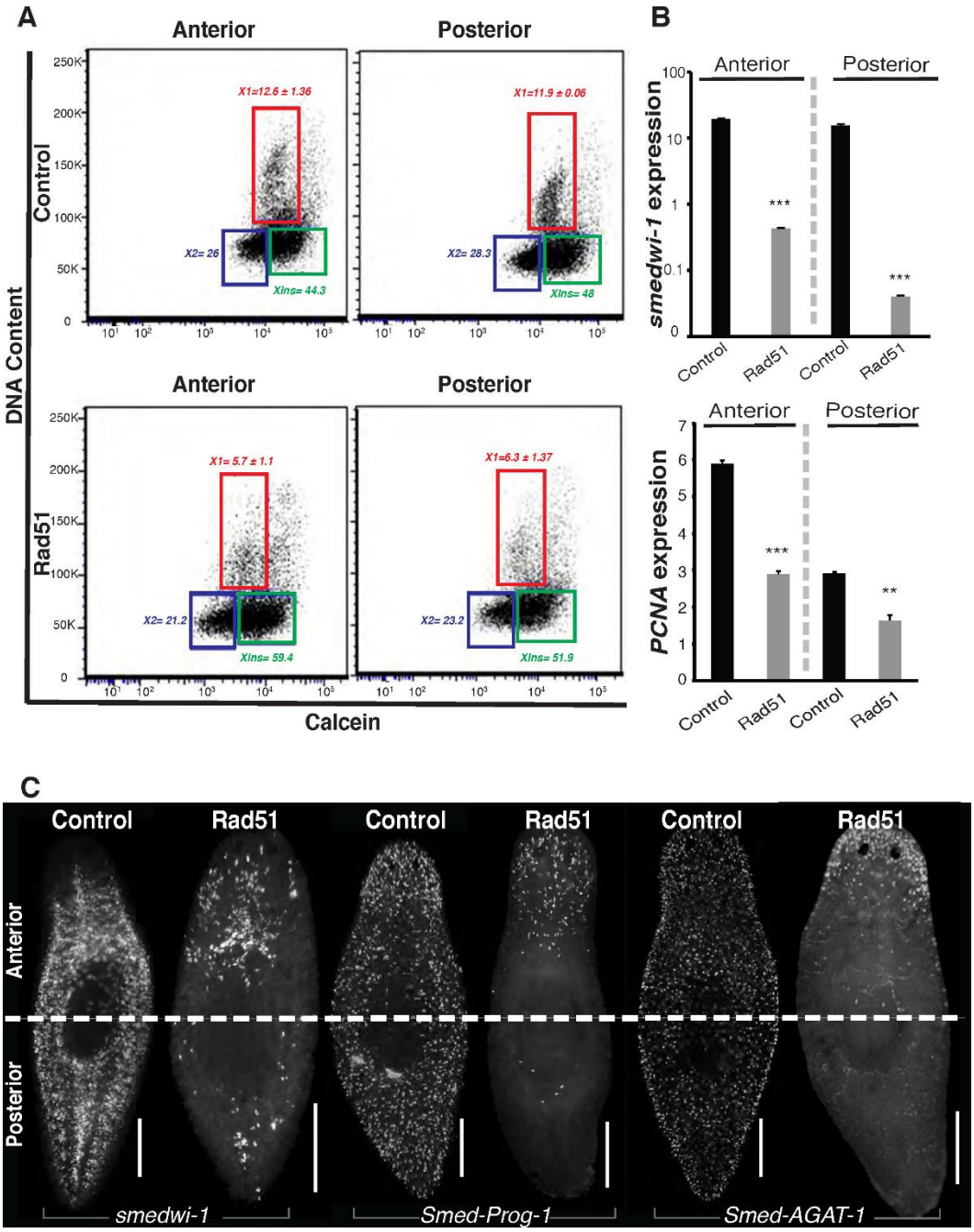

Fig. S4. Systemic Rad51 dysfunction impairs neoblasts and their division progeny. (A) Flow cytometry analysis using Draq5 as the DNA content marker and calcein as the live cell marker shows reduction in the proliferative neoblasts (X1 population) after *Rad51(RNAi)*. The difference in the frequency distribution is statistically significant between different regions of control and *Rad51(RNAi)*, anterior (*P=0.016*) and posterior (*P=0.014*), respectively. For simplicity the extended values for X2 and Xins cells are not shown. **(B)** Gene expression levels of neoblast markers *smedwi-1* and *Smed-PCNA* in anterior and posterior regions of control and *Rad51(RNAi)* animals. **(C)** Whole-mount fluorescent in situ hybridization staining with markers of neoblasts (*smedwi-1*) and their early (*Smed-Prog-1*) and late (*Smed-Agat-1*) progeny. All analyses were performed on intact animals ~30-35 days after first dsRNA injection. All graphs/plots represent mean ± s.e.m. of three or more independent experiments with n=5-10 animals per experiment. Gene expression values represent mean±s.e.m. of triplicates per experiment and at least three biological replicates, each condition was generated by extracting RNA from >20 animals. The internal control is the ubiquitously expressed clone *H.55.12e*. All graphs represents mean±s.e.m. of at least three biological replicates with *n>10* animals per experiment. ****P<0.0001* and ***P=0.004* by Tukey's multiple comparison test. Scale bar, 200 µm.

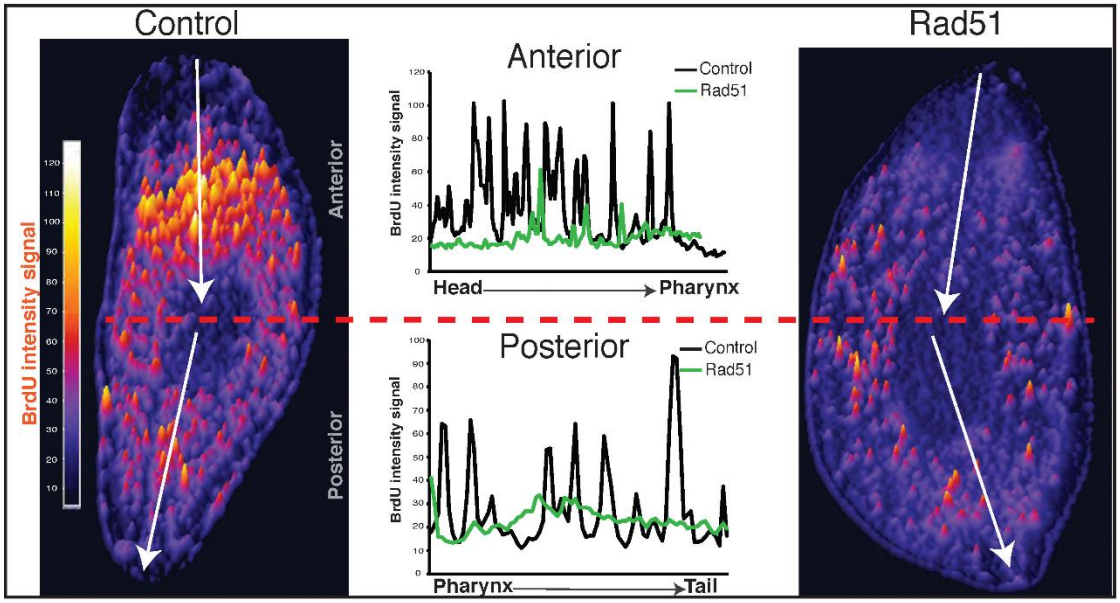

Fig. S5. **The bromodeoxiuridine analog (BrdU) is asymmetrically incorporated along the AP axis.** The intensity of BrdU signal was obtained across the midline of intact (uninjured) controls and *Rad51(RNAi)* animals. Higher levels of the signal are designated with yellow-white and lower levels of intensity are represented by purple color (scale bar on the left). Individual intensity plots are presented for anterior (i.e. head-pharynx, top) and posterior (i.e. pharynx-tail, bottom) region for both control and the experimental group. Intensity of the BrdU signal was calculated with Image J software by drawing a line through the middle of the picture to generate an intensity profile (white arrow). For consistency these are the same pictures found in Figure 3I. However, results show similar tendency in the BrdU intensity across two independent experiments, *n=5* animals each.

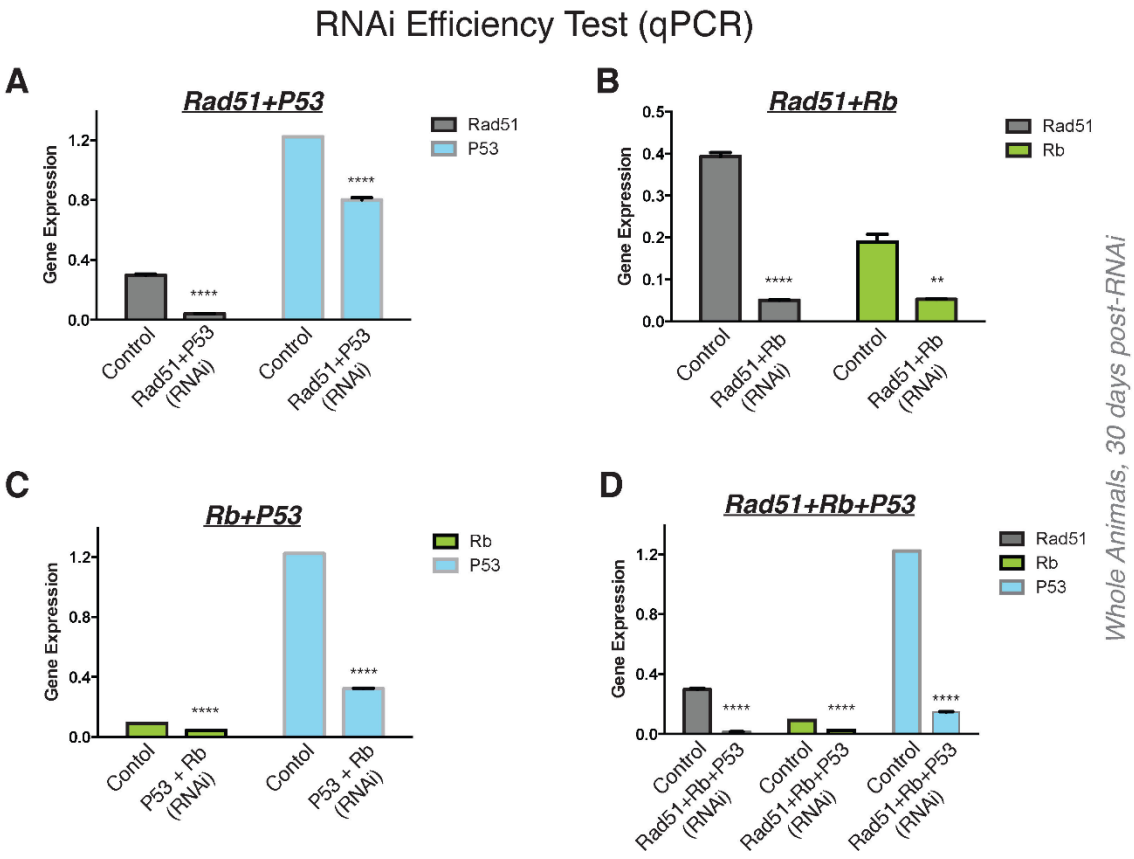

Fig. S6. **Simultaneous downregulation of gene expression with multiple RNAi.** The RNAi efficiency of the RNAi protocols was tested with quantitative PCR (qPCR). (**A-D**) show gene expression for each gene after double and triple downregulating of Rad51, Rb, and p53. RNA was extracted from whole animals subjected to double and triple RNAi after 30 days of the first injection (the particular genes targeted with dsRNA are shown at the top right of each graph). In all cases the RNAi strategy significantly downregulated the expression of the targeted genes ***P<0.001*; *****P<0.0001* by One Way Anova. The average RNAi efficiency is slightly lower in triple RNAi (~80% vs 90% in double RNAi) but there was no difference in the timeline and dynamics of the phenotype at the macroscopic and microscopic levels (not shown). Gene expression values represent mean±s.e.m. of triplicates per experiment and at least three independent experiments, each condition was generated by extracting RNA from >20 animals. The internal control is the ubiquitously expressed clone *H.55.12e*.

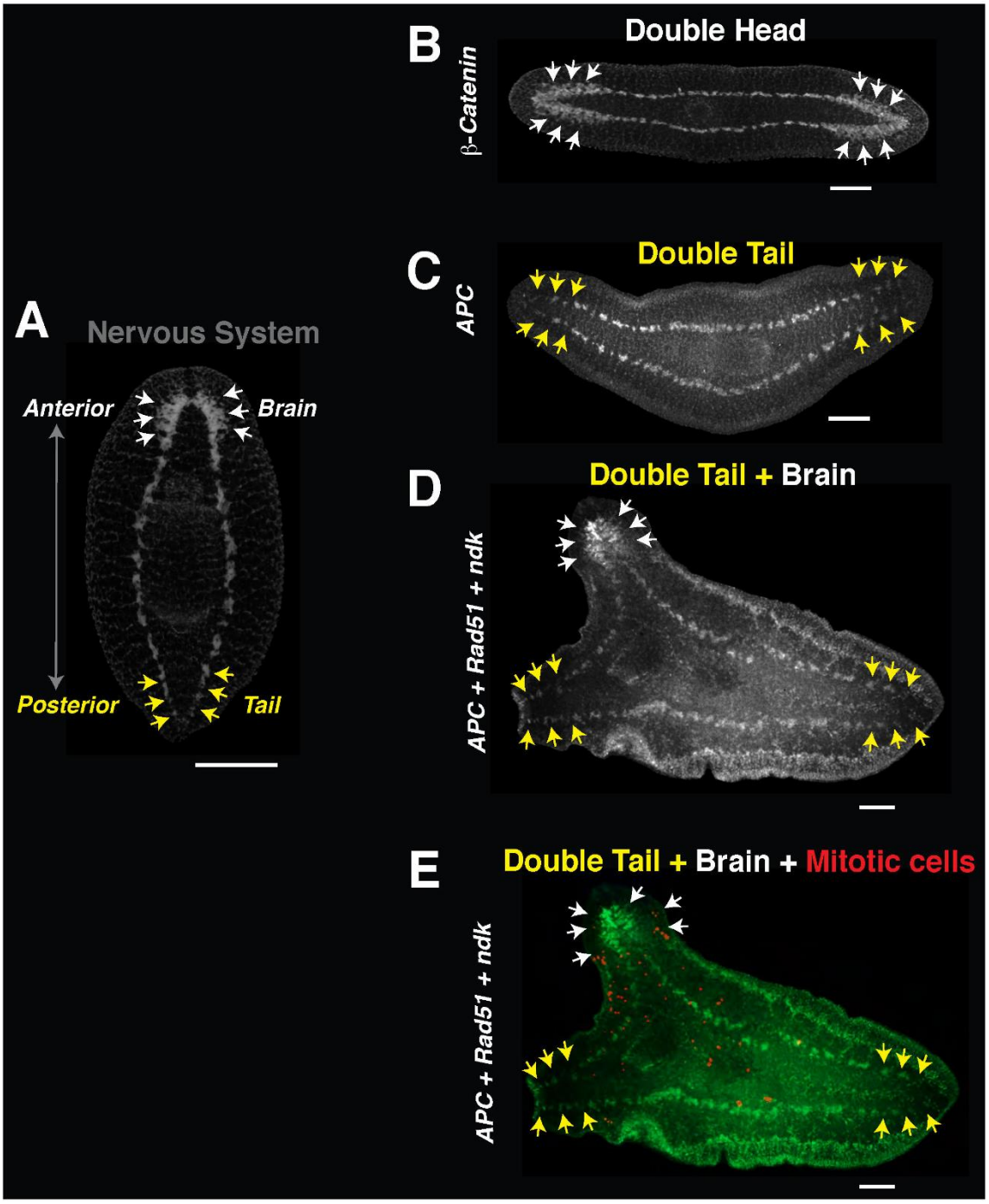

Fig. S7. **Anterior specific nervous tissue modulates cell division in posteriorized animals. (A)** Nervous tissue in planarians is labeled with anti-synapsin antibody (gray signal), which shows accumulation of neurons in the anterior area (cephalic ganglia, for simplicity: brain indicated white arrows) and parallel neural projections that reach the posterior area (ventral nerve cords, VNC, yellow arrows). **(B)** Double headed organism generated by downregulation of *ß-catenin* signaling, note brain tissue at each end of the animal (white arrows). **(C)** RNAi of the *adenomatous polyposis coli (APC)* gene leads to animals that lack brain tissue and display double tail morphology (yellow arrows). **(D)** Triple RNAi involving *APC + Rad51 + nou-darake (ndk)* generates double tail organisms with ectopic brain tissue (white arrows) in which cell division is associated to the proximity of brain tissue (**E**, red signal). Scale bar, 200 µm.

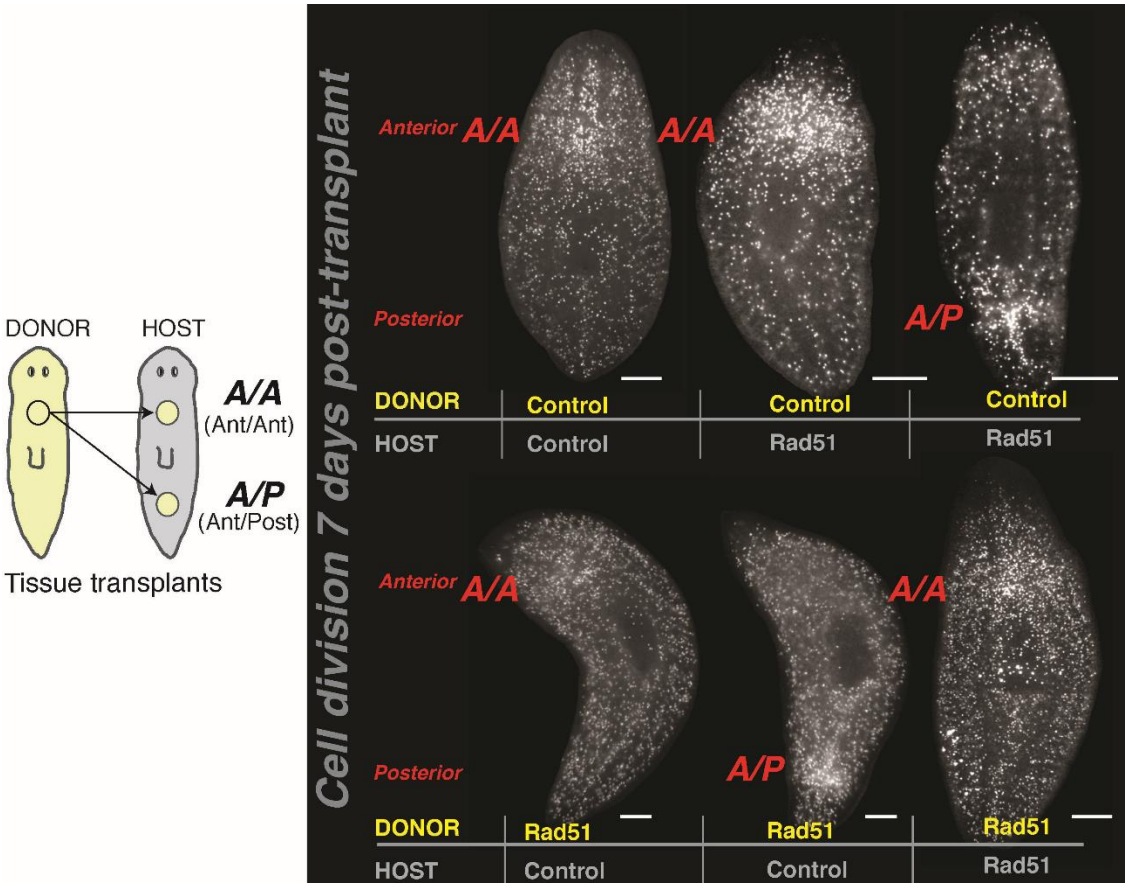

Fig. S8. **Tissue transplants from Rad51 donors lead to hyperproliferation.** Whole-mount immunostaining labeling mitotic activity with the H3P antibody (white dots) one week after tissue transplants were engrafted in either anterior or posterior parts of the animals. Schematic representation of tissue plug transplants from the anterior region of donor animals into host animals (left side), indicated with arrows (*A/A*=anterior to anterior, or *A/P*=anterior to posterior). Donor tissue from control animals was able to re-establish mitotic activity on Rad51 hosts (top row). However, tissue transplanted from Rad51 donors, always led to systemic hyperproliferation (bottom row). All transplants were carried out at 30 days after first dsRNA injection and the images are representatives of two independent experiments, $n>5$ animals each. Scale bar, 200 µm.

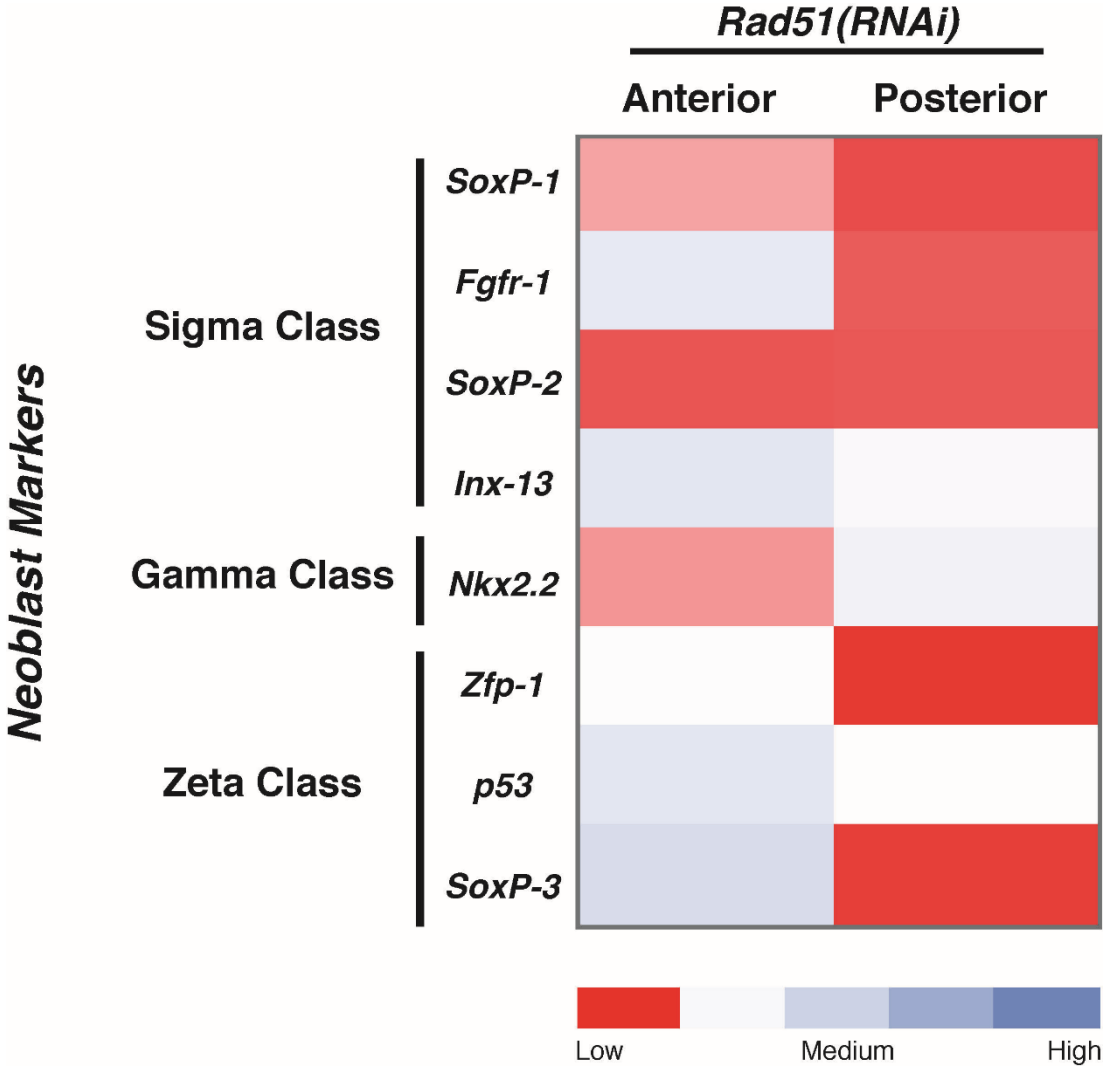

Fig. S9. Rad51 is required for proper expression of neoblast markers. Heat map representation of gene expression levels of neoblast markers in the anterior or posterior regions from the *Rad51(RNAi)* condition with respect to control. Overall, gene expression among different subpopulations of neoblasts (Sigma, Gamma and Zeta) was downregulated but markers of the Zeta class in the anterior region were less impacted than the other neoblast types. The red and blue colors represent fold changes in gene expression levels. Gene expression correspond to the mean of triplicated samples of at least two biological replicates with pooled RNA extraction of >20 animals each. X1 cells serve as the source of RNA in two independent experiments.

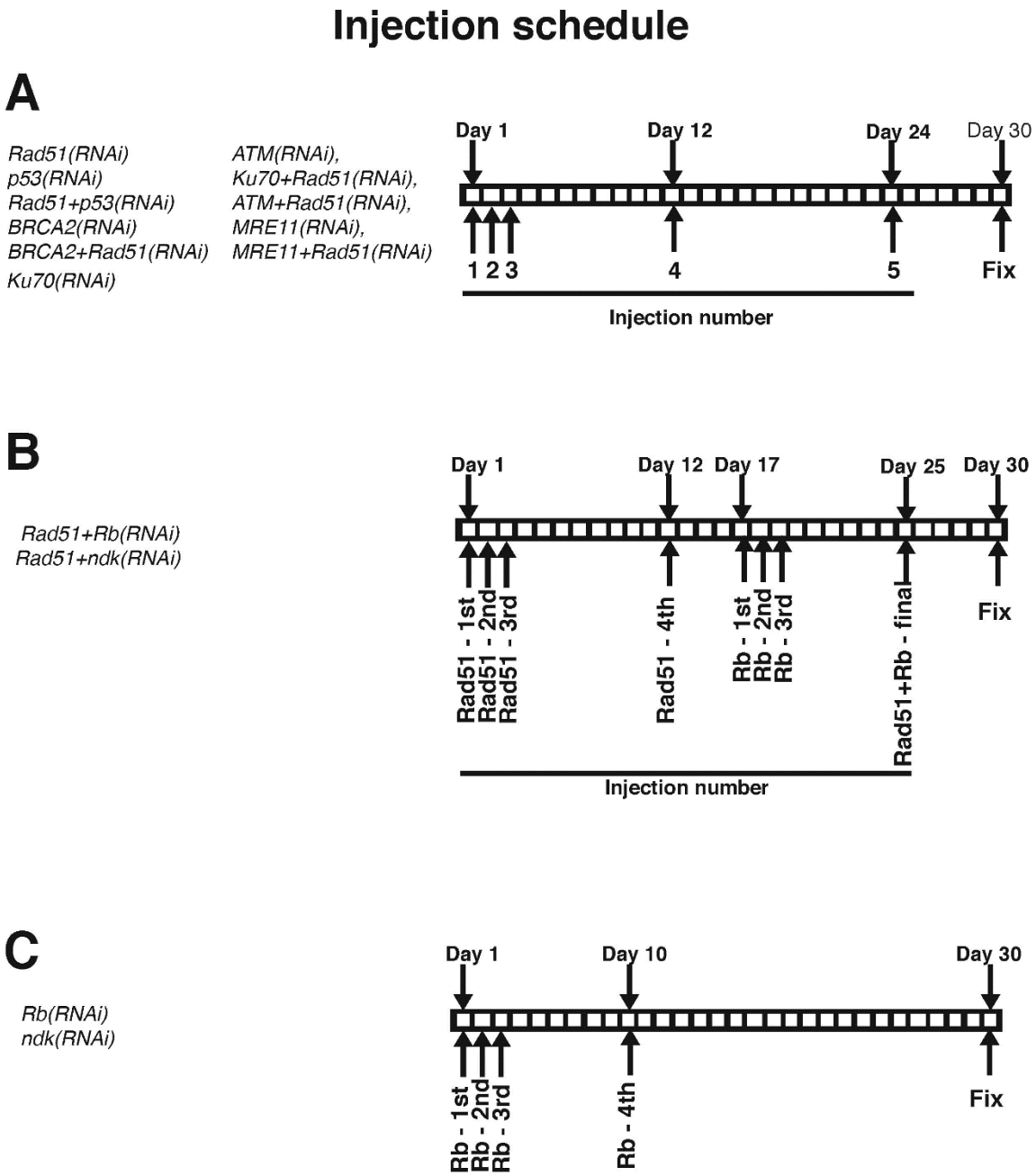

Fig. S10. **dsRNA microinjection schedule. (A, B, C)** Schedule to downregulate genes listed on the left with a total of 4-8 microinjections as illustrated in the lower part of each timeline. Animals were processed 30 days post first injection or at least 4 days after the last injection.

Table S1. List of primers and probes used in this study.

Oligos used for cloning genes and probes		
Name	Forward Primer	Reverse Primer
Rad51	TTTGCAAGGTGGTGTTGAAA	ATCAGCCAACCGTAACAAGG
Ku70	AGGCATGAAATTGGACGAAG	CGACTAGGAGGAGGTGATCG
MRE11	GCATGCAGCGAAGAATTACA	ATCGGATCAATGGCAAAGTC
ATM	GGTTTTGCTTCACGATCCAT	ATCGCAGAAACCAGAGCAGT
Rb	ATGGCGGAGTCAATTTCAAC	GCAATTCGAGAACCTCAAGC
P53	CCTGCTTTTAAATCCGACGA	AAGTGTTTTCCGACCACCTG
BRCA2	ACGATTTACCACCCGAATCA	CGTGAACGTGTCAACAAACC
RPA	GAATCGGACGTCCATGAGAT	GCGGCTGAAATGGAGAAATA
ndk	GAAATTAACGAAGCCCGTCA	TCCCTTTTCACTTTCC
Oligos used for qPCR		
Name	Forward Primer	Reverse Primer
Rad51	ATGTCAGAATCCCGATACGC	ATCAGCCAACCGTAACAAGG
Ku70	TAGTTGGCATTGGGATCCAT	CAGATTTGTGCTGCCTTCAA
MRE11	GCTGGCAACGACTAAGGAAC	CCCGATATATTCCTGGCTGA
ATM	CTGATTGGTCGGCTTTCATT	AGCTAACCAATCCCCCAAAG
Rb	CCACGAGATCCTCCAAATGT	CGTGTGAACATTGGTTTTGC
BRCA2	CAAAGAGACCCTGCTTGAGG	AGCCGGAACACAGTACCATC
UDP	TTCCTACAGCCACTTGAGCGAC	GTCGGTGGTTATTTTGCG
Smedwi-1	TTTATCGTGACGGTGTTGGA	TTGGATTAGCCCCATCTTTG
NB.21.11e	GCAGATGACGTGAAACAAGG	TACTTGATTTGGCGGGAGAC
Agat-1	ACCGATTCCAGTTTCGCTTA	TCAATCGCTCCAAAATCTCA
Cyclin B	TCGGGAAATAGTTCGAATGC	CCAAGGACATCGCAGAAAAT
Soxp-1	TGGTTGGACGTCGCCTTCTT	ACCCATTACCTCCTGAATGGCT
Fgfr-1	CGGCATCCAATAAGTGCGCT	TGTCAGTTTCAGTGGGAACTCCA
Soxp-2	CTTCCCAAGAAGTTTGCTTATTTCTGA	GGCCATTGAATAGTTTCATGATATTTTCCA
Inx13	AAACGGAATCCATTGGTAATAATTCATTCT	GCTGGGTTGAAGGCACTGTT

Nkx2.2	TCGCCAAATTATGCTCAGATTGATCC	CGATTTCTTGTTCACTGGAATTCGGA
Zfp-1	CCCGTGCCTGAACAATTTGACA	CCTCAGCGCATGCCTCTGTA
P53	TGGTTGCATTGCATCGGAACA	GGCCCAGCAATATATTACTTCGGC
Soxp-3	TGTGGTTGGAATTTTTCACTGATTTCT	ACCTGTGCAGACAATTCGAAGA